Biochemistry and Biophysics Reports 19 (2019) 100657

Contents lists available at ScienceDirect

Biochemistry and Biophysics Reports

journal homepage: www.elsevier.com/locate/bbrep

Role of sunscreen formulation and photostability to protect the biomechanical barrier function of skin

Christopher Berkey[a], Nozomi Oguchi[b], Kazuyuki Miyazawa[b], Reinhold Dauskardt[a,*]

[a] Department of Materials Science and Engineering, Stanford University, Stanford, CA, 94305-2205, USA
[b] Shiseido Co., Ltd, Advanced Technology Research Group, Global Innovation Center, 2-2-1, Hayabuchi, Tsuzuki-ku, Yokohama, 224-8558, Japan

ARTICLE INFO

Keywords:
Sunscreen formulation
Skin barrier function
Corneocyte cohesion
UV light damage
Stratum corneum

ABSTRACT

The impact of sunscreen formulations on the barrier properties of human skin are often overlooked leading to formulations with components whose effects on barrier mechanical integrity are poorly understood. The aim of this study is to demonstrate the relevance of carrier selection and sunscreen photostability when designing sunscreen formulations to protect the biomechanical barrier properties of human stratum corneum (SC) from solar ultraviolet (UV) damage. Biomechanical properties of SC samples were assayed after accelerated UVB damage through measurements of the SC's mechanical stress profile and corneocyte cohesion. A narrowband UVB (305–315 nm) lamp was used to expose SC samples to 5, 30, 125, and 265 J cm^{-2} in order to magnify damage to the mechanical properties of the tissue and characterize the UV degradation dose response such that effects from smaller UV dosages can be extrapolated. Stresses in the SC decreased when treated with sunscreen components, highlighting their effect on the skin prior to UV exposure. Stresses increased with UVB exposure and in specimens treated with different sunscreens stresses varied dramatically at high UVB dosages. Specimens treated with sunscreen components without UVB exposure exhibited altered corneocyte cohesion. Both sunscreens studied prevented alteration of corneocyte cohesion by low UVB dosages, but differences in protection were observed at higher UVB dosages indicating UV degradation of one sunscreen. These results indicate the protection of individual sunscreen components vary over a range of UVB dosages, and components can even cause alteration of the biomechanical barrier properties of human SC before UV exposure. Therefore, detailed characterization of sunscreen formulation components is required to design robust protection from UV damage.

1. Introduction

Solar ultraviolet (UV) radiation is well known to have salutatory effects on the body such as stimulating the production of vitamin D. However, it is important to consider that during UV exposure *in vivo* these effects are multi-faceted. Within the dermis, the production of abnormal elastotic tissue along with the breakdown of the collagen network are both known effects of UV damage, likely resulting from the up-regulation of matrix metalloproteinases (MMPs) due to reactive oxidative species (ROS) generation by UV [1,2]. Additionally, both single large acute doses and low levels of repeated UV radiation have been shown to induce hyperplasia within the epidermis and stratum corneum due to modulation in the expression of genes controlling the differentiation and proliferation of keratinocytes [3,4]. The increased production of keratinocytes has been linked to skin surface alterations such as changes in hydration, skin topography, and epidermal thickness, all of which would affect the skin barrier function [3,5].

While these multi-faceted effects occur throughout all skin layers, our work focuses specifically on the impact of UV radiation on stratum corneum (SC) damage processes and barrier function. Since the SC is comprised of fully differentiated corneocytes without nuclei or organelles, our *in vitro* analysis of UV effects on the SC barrier function yields good insight into the same *in vivo*. In fact, it is UV damage to the mechanical behavior of the SC layer which leads to the greatest loss of mechanical integrity in full-thickness tissue [6]. This is because although the collagen and elastin extracellular matrix of the dermis controls the macroscopic deformation of skin, the SC dominates the local biomechanical behaviors and stress levels of full-thickness skin (including damage processes and tactile perception) due to its much greater stiffness compared to that of deeper skin layers [6–9].

UV radiation has deleterious effects on the biomechanical barrier properties of SC, ultimately reducing the SC barrier function and

* Corresponding author.
E-mail addresses: caberkey@stanford.edu (C. Berkey), nozomi.oguchi@to.shiseido.co.jp (N. Oguchi), kazuyuki.miyazawa@to.shiseido.co.jp (K. Miyazawa), rhd@stanford.edu, dauskardt@stanford.edu (R. Dauskardt).

https://doi.org/10.1016/j.bbrep.2019.100657
Received 21 March 2019; Received in revised form 2 May 2019; Accepted 4 June 2019
Available online 10 June 2019

undermining its ability to provide robust physical and chemical protection for the body from the environment [5,6,10,11]. UV radiation weakens the mechanical stability of the skin by increasing the inherent mechanical stress within the SC that is the driving force behind cracking and chapping, as well as damaging the cohesion energy of the SC (its resistance to cracking and chapping) [6,12]. Consequently, the barrier function of the SC is greatly impaired and more susceptible to further degradation after the biomechanical properties of the SC have been damaged by UV radiation. It is important to note that the SC exhibits remarkable resistance to UV degradation such that generally large UV doses as part of an accelerated testing technique are required to elicit the full extent of cohesive damage [6]. However, there is a growing body of evidence which suggests frequent low level doses of UV radiation *in vivo* may have a cumulative effect on skin health similar to fewer acute doses [5,13].

In recent publications, we introduced a suite of *in vitro* thin-film mechanics techniques capable of precisely quantifying the mechanical barrier properties of human SC when exposed to chemical treatments or changes in temperature [7,8,14–16]. We have also demonstrated the ability of these techniques to measure the effects of UV radiation on the SC as well as the efficacy of sunscreens in preventing UV damage to the barrier properties of human SC [6,12]. Here we demonstrate the versatility and precision of these techniques by comparing the photostabilities of octyl methoxycinnamate (OMC), a commonly used organic UVB absorbing molecule, and dioctyl 4-methoxybenzylidene malonate (DOMBM), a more novel molecule designed to have a higher photochemical stability for use in commercial sunscreens.

In the evaluation of sunscreen efficacy for protecting the barrier function of human SC, the photostability of sunscreens is a critical factor. Many sunscreen molecules lose their UV filtering efficacy due to photochemical reactions that occur during solar exposure [17,18]. Not only does this leave the skin unprotected from further UV radiation damage, but in some cases the byproducts and intermediates of these reactions are reactive oxidative species (ROS) or other cytotoxic molecules which can sensitize and further damage the skin well before full degradation of the sunscreen [19–21]. Our accelerated UV damage procedure clarifies differences in sunscreen stability that may not be readily apparent at lower dosages, but which have a large impact on ROS burden on the skin at any radiation level. This problem of low photostability is common even in commercially available sunscreens, highlighting the need for standardized and robust photostability measurements [18,22].

Adequate protection of the SC from UV degradation requires sunscreens that are not only screened for a high initial UV filtering capacity, but that are also appropriately tested to ensure high photostabilities. As the SC is the main diffusion barrier of the skin, most inorganic and chemical sunscreens only interact with the SC without reaching deeper layers of the skin [23–25]. OMC in particular has been shown to have extremely low penetration capability through the SC [26,27]. Thus, studying the effects of sunscreen treatments and accelerated UV exposure on the biomechanics of isolated SC *in vitro* has very significant *in vivo* relevance, since the structure of the SC is maintained during isolation from full-thickness tissue.

Here we implement our suite of thin-film mechanics techniques to systemically compare the photostabilities of two similar sunscreens, octyl methoxycinnamate (OMC) and dioctyl 4-methoxybenzylidenemalonate (DOMBM), while also evaluating their efficacies at preventing UVB damage to the mechanical barrier properties of the skin. The results illustrate the importance of sunscreen photostability in protecting the biomechanical characteristics of the SC, as well as strength of our techniques at evaluating precise differences in sunscreen behavior.

2. Materials and methods

2.1. Stratum corneum preparation

Full-thickness samples of cadaverous human skin were obtained through the National Disease Research Interchange (NDRI). The SC was isolated from these full-thickness abdominal samples through a trypsin-digest process described previously [6]. All abdominal tissue was stored in a −80 °C freezer until processing. After cutting away subcutaneous tissue, the epidermis was separated from the dermis via heat treatment in 35 °C water for 10 min immediately prior to a one minute soak in 60 °C water, followed by mechanical separation using a flat-tipped spatula. The underlying epidermal tissue was then removed from the SC by floating the tissue in a trypsin enzymatic digest solution [0.1% (wt/wt) in 0.05 M, pH 7.9 Tris buffer] at 35 °C for 180 min. The SC was then rinsed and allowed to dry on filter paper (medium flow, grade 995 filter paper; Whatman), and then removed to be stored in a low-humidity chamber (~10–20% RH) at an ambient temperature of ~18–23 °C. Direct comparisons of absolute SC stress profiles and cohesion energies were only made between specimens from the same donor tissue sample, in order to control for variations that may occur in phototype between donors. Percent changes in normalized peak drying stresses were compared between two different donor samples to more effectively characterize differences in sunscreen efficacy.

2.2. UV exposure and sunscreens

The sunscreens used in this study were the UVB absorbing molecules octyl methoxycinnamate (OMC) and dioctyl 4-methoxybenzylidenemalonate (DOMBM). OMC is a well-known UVB filter that is widely used in commercial sunscreen formulations [27–29]. OMC has also been included in more complex treatment formulations to broaden UVB protection or as a stabilizing ingredient meant to absorb certain UVB wavelengths in order to prolong the lifetimes of other sunscreen molecules [30,31]. However, recent publications have shown that DOMBM, a novel UVB absorber without isomers, may have significantly enhanced photostability compared to OMC, which is known for its low stability due to isomerization [31,32]. These molecules were chosen to highlight the ability of our thin-film measurement techniques in characterizing precise differences in the photostability profiles of sunscreens with regards to the mechanical stability of the SC. The OMC and DOMBM were always applied in the commercially available and widely used carrier molecule glyceryl tri-2-ethylhexanoate (GTE) at a concentration of 8 wt%. GTE is often used as an emollient in cosmetic skin treatments, and we have recently reported its basic effect on stresses in the SC [33].

Since OMC and DOMBM are UVB absorbing molecules, all samples were exposed to narrowband UVB radiation (305–315 nm) in order to best compare the efficacy and photostability of these sunscreen molecules using our suite of thin-film mechanics techniques. Additionally, maintaining a robust defense against UVB radiation is critical because although UVB radiation is a smaller portion of incident solar UV radiation compared to UVA radiation, it is more energetic than UVA radiation and it is responsible for most cases of erythema and direct damage to the DNA of epidermal cells [5,34]. All UVB radiation was produced by a commercial phototherapy system (SolRx 100; SolarC Sytems) using a 9W narrowband UVB lamp (PL-S 9W/01/2P; Philips). The measured irradiation spectrum of this Philips lamp is shown in Fig. 1 plotted with the ASTM standard solar irradiance spectrum at ground level with a 37° hemispherical tilt [35]. The peak irradiance of the lamp occurs between 307-315 nm and all wavelengths produced by the lamp are present in the solar spectrum at ground level. The lamp power output in the narrowband UVB region is ~7 times greater than solar power output in this region, which is useful and necessary to accelerate damage in the SC and decomposition processes in the sunscreens studied. Various amounts of narrowband UVB exposure

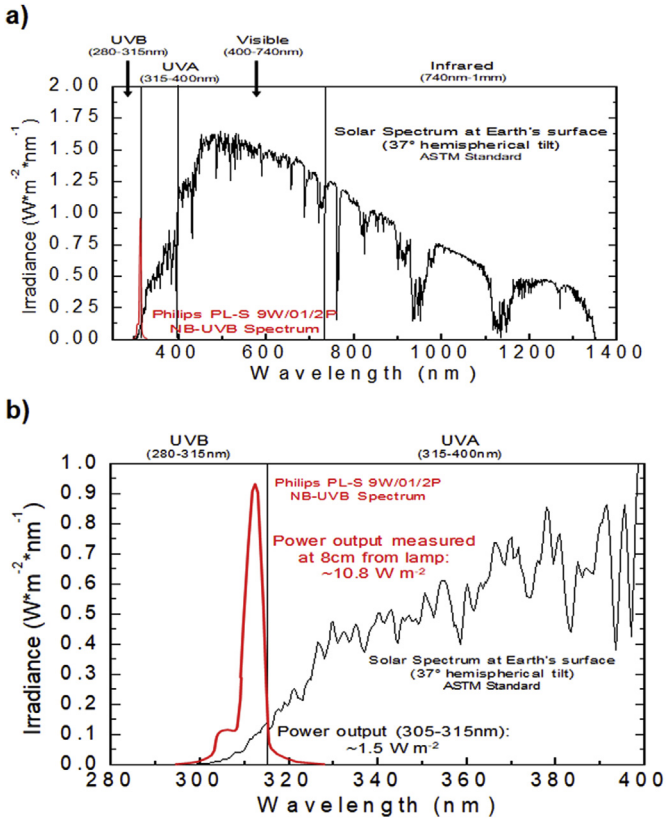

Fig. 1. The ASTM standard solar irradiance at Earth's surface with 37° hemispherical tilt [35] overlaid with the Philips PL-S 9W/01/2P narrowband UVB bulb spectrum at wavelength range **(a)** 280-1400 nm and **(b)** 280-400 nm.

were chosen during this accelerated damage study to fully characterize the filtering efficacy and photostability of the OMC and DOMBM molecules (as well as their carrier compound). For drying stress measurements, specimens were exposed to 0, 5, 30, 125, and 265 J cm^{-2} of narrowband UVB radiation. Similarly, for dual-cantilever beam experiments, after one of the treatments of interest was applied, specimens were exposed to 0, 125, and 265 J cm^{-2} of narrowband UVB radiation. The 5 and 30 J cm^{-2} conditions were included in drying experiments to characterize the behavior of treatments in a more physiologically relevant range of UVB exposure amounts, as these conditions correspond to ~10 h and ~60 h respectively of uninterrupted solar narrowband UVB exposure [35]. We have chosen these large UVB dosages to amplify tissue response in an accelerated damage test such that the maximum damaging effects of UVB on the mechanical properties of SC would be observable. We believe this has physiological relevance for two key reasons. First, by measuring changes in sunscreen efficacy at large UV dosages, we can extrapolate information concerning sunscreen behavior at lower dosages where partial degradation may present a critical issue of generating ROS [19–21]. Second, emerging evidence suggests small UV exposures may accumulate to effect greater damage in the skin [5,13].

Immediately prior to all UVB exposures, an average amount of treatment of 2.7 mg cm^{-2} for cohesion specimens or 2.2 mg cm^{-2} for drying stress specimens was applied directly on the SC surface using a wooden dowel to ensure a relatively even layer. These amounts were somewhat higher than the commercial standard of 2.0 mg cm^{-2} to allow for more complete and even coating of the SC after it had been adhered to substrates, which is necessary for accurate biomechanical measurements. During exposure to UVB radiation, specimens were kept in an environmental chamber (LH-06 Humidity Chamber; Associated Environmental Systems) held at 40% RH and 25 °C in order to simulate typical ambient conditions while preventing local humidity or temperature fluctuations. In dual-cantilever beam experiments (described below), sunscreen formulation treatments and UVB exposures occurred only once before the first delamination and were not repeated for subsequent delaminations.

2.3. Drying stress profiles

In a process described previously in Ref. [16], the drying stresses in SC were measured by monitoring the curvature of a glass substrate onto which the SC had been adhered. In order to relate the drying stress of the SC, σ_{SC}, and the elastic curvature of the substrate, K, Stoney's equation was used:

$$\sigma_{SC} = \left(\frac{E_{sub}}{1-\nu_{sub}}\right)\left(\frac{h_{sub}^2}{6h_{SC}}\right)K \quad (1)$$

where E_{sub}, ν_{sub} and h_{sub} are the Young's modulus, Poisson's ratio, and thickness of the substrate, respectively. The initial and final thickness values of the SC, h_{SC}, were measured with a digital micrometer. SC thickness was assumed to vary linearly with time from initial stress onset until the stress reached a constant (plateau) value. The SC was assumed to be a "thin film" compared to the substrate. This assumption is valid since the product of the film biaxial modulus and thickness are easily $\leq$1/80th of the equivalent product for the substrate. This assumption is quite useful since it means that the elastic properties of the film are not required. SC that had been fully hydrated by submersing in water for 25 min was adhered to 22 mm × 22 mm x 177 mm borosilicate glass coverslips (12–541- B; Fisher Scientific) with reflective Cr/Au (35 Å/465 Å) films deposited on one surface. Slippage of the SC does not occur, due to interactions between SC protein components and the borosilicate glass. A study from our group has addressed this previously [8]. In the present study, to prevent any possibility of slippage, a very thin layer of cyanoacrylate adhesive was applied to sample edges after the wet SC was adhered normally. Experiments showed this did not affect measured values of mechanical stresses within the SC (data not shown). The curvature of the borosilicate glass was then measured using a substrate curvature instrument (FLX-2320; Tencor Instruments), with ambient temperature and humidity controlled at < 5% RH. The instrument operates by using a laser to scan and determine angle of deflection across the substrate, thus measuring an average curvature value. After the plateau stress was reached, the specimen was placed in the environmental chamber at 40%RH for two hours to rehydrate to ambient moisture levels before applying sunscreen formulations or exposing to UVB radiation. After being treated or UVB exposed, the specimen was placed in a 99%RH chamber for two hours to fully hydrate before another drying stress measurement was performed.

2.4. Corneocyte cohesion

Corneocyte cohesion tests were performed following the procedure described previously [6]. The double-cantilever beam (DCB) test geometry was implemented. Using cyanoacrylate adhesive, SC was initially adhered between two elastic substrates of polycarbonate. To enable the use of linear elastic fracture mechanics to determine strain energy release rates, substrate dimensions of 40 × 10 × 3 mm^3 were chosen. This ensured the substrates underwent purely elastic deformation during testing. Loading tabs were used to mount the specimens in a micromechanical adhesion testing system (Delaminator v8.2; Dauskardt Technical Services). The system operated with a computer-controlled DC servoelectric actuator in displacement control mode to propagate a debond path through the SC layer. The displacement rate was set to 2.0 μm s^{-1} at the beginning of the test and was incrementally increased by 2.0 μm s^{-1} throughout the test up to a maximum of 8.0 μm s^{-1}. The load-versus-displacement curves generated via analysis with the DTS Delaminator were used to determine specimen compliance, which enables calculation of the debond length. The cohesion energy, or G_C, was

then found by implementing the following equation derived from linear elastic fracture mechanics:

$$G_C = \frac{P_C^2}{2b}\left(\frac{dC}{da}\right)\Big|_{a_C} \quad (2)$$

where P_C and a_C are the critical load and critical debond length at crack propagation, respectively, b is the substrate width, C is the compliance of the specimen, and a is the debond length. For the symmetrical DCB geometry, compliance is given by:

$$C = \frac{8(a + 0.64h)^3}{E'bh^3} \quad (3)$$

where E' is the reduced substrate modulus and h is the substrate thickness. The factor added to the debond length is a correction factor first described by Kanninen [36].

To perform graded cohesion tests, a substrate beam with delaminated tissue from the original specimen would be adhered to a fresh substrate beam to delaminate the remaining SC layers. Before the first delamination, and after every subsequent delamination, the thickness of the SC and its substrate beam was measured in five locations along the length of the beam using a micrometer (Micrometer 293-348-30; Mitutoyo). Thus, we characterized the average thickness change corresponding to each delamination, which is directly related to the depth beneath the SC surface at which each delamination occurred. In this way, we were able to generate scatter plots of cohesion energy versus depth into the SC. We then performed a linear fit on each set of delaminations and extrapolated G_C values at 2, 4, and 6 μm for all data sets. These depth-fitted data sets allow for direct comparison of G_C values obtained while testing the effects of different treatments and UVB exposures. A linear fit was chosen in light of previously published results that indicate the cohesion energy of SC increases linearly near the skin surface before beginning to grow exponentially at deeper SC layers [14]. The cohesion energies reported here are all extrapolated from linear fits in this way. For all testing conditions, three to five specimens prepared from the same tissue sample were tested with a percent yield of 73%. An average of ten cohesion energies were obtained per specimen, for an average of n = 27 per test condition. Error bars shown in figures represent the standard error of these data sets.

3. Results and discussion

3.1. Drying stress profiles after carrier treatment and UVB exposure

Results of drying stress measurements performed on sunscreen treated and untreated SC, including peak stress changes due to increasing UVB dosages as well as complete drying stress profiles, are shown in Fig. 2 (Fig. 2a, b, c). The mechanical stresses that develop within the SC are of critical importance in understanding the skin barrier function, as a higher inherent state of stress within the SC is a driving force for cracking, chapping, and other mechanical damage [6,8]. It is important to note that changes in mechanical stress in the SC not only impact the damage characteristics of skin, but also human perception of skin stiffness or tightness, making drying stress a key metric in skin protection [16].

We measured the mechanical stress of SC during drying before and after exposure to 265 J cm^{-2} of UVB radiation and found that the peak stress value increased by nearly 23% (Fig. 2a). This is consistent with past studies detailing the increase in stress within SC due to UV radiation [6,12]. Since drying stress is fundamentally caused by water loss, which is known to be controlled by the lipid interlayer of the SC [16,37,38], it is likely that UV radiation leads to an increased stress in SC by damaging the lipids within the skin allowing a greater volume of water to be lost. In fact, UV radiation has been shown to both disrupt the lamellar organization of intercellular lipids within the SC and also generate ROS which in turn degrade SC lipids through peroxidation

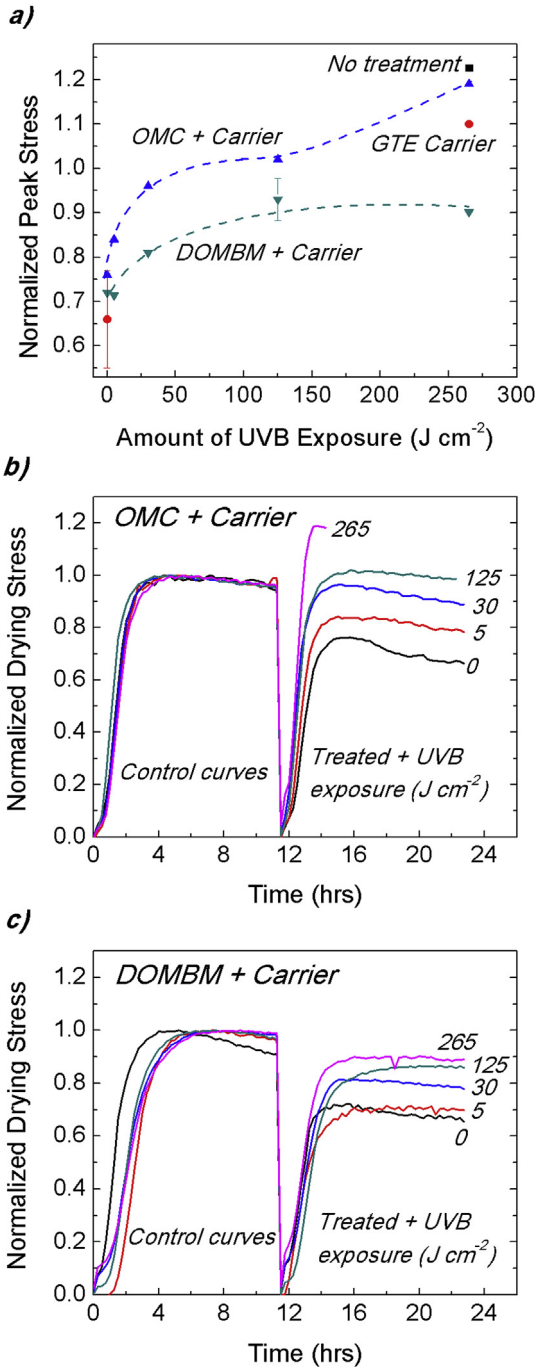

Fig. 2. (a) Comparison of peak stresses observed during drying stress experiments performed on SC treated with the OMC and DOMBM formulations and exposed to 0, 5, 30, 125, 265 J cm^{-2}of UVB radiation. Also reported are the peak stresses of untreated tissue, as well as SC treated with the pure GTE carrier, which was measured after 0 and 265 J cm^{-2} UVB exposures. Normalized biaxial film stresses for SC films treated with the GTE carrier containing **(b)**8 wt% OMC or **(c)**8 wt% DOMBM and exposed to 0, 5, 30, 125, 265 J cm^{-2} of UVB radiation. Pre-treatment control curves are shown on the left. Curves were normalized relative to the peak stress of each control curve.

reactions, effects which would explain a greater total water loss during drying [39–41].

Peak stress observed within SC treated with the GTE carrier decreased by 34% with no UVB exposure (Fig. 2a). These results suggest that in the absence of UVB radiation, the GTE carrier reduces the amount of water lost from the SC during drying. This may indicate that the GTE carrier is a humectant molecule which interacts strongly with

water, thus preserving SC hydration in a dry environment. However, this explanation is inconsistent with cohesion data discussed later in this work and seems unlikely given the presence of relatively hydrophobic side groups in the GTE molecule. Another possible explanation is that the GTE carrier strongly interacts with lipids covalently bound to corneocytes, forming a more compact hydrophobic diffusion barrier to water in the SC and reducing total water loss. Increased lipid compaction has been previously observed when bound lipids are shifted into close proximity with each other to increase interactions [14,42]. The impact of OMC and DOMBM sunscreen formulations on stress was also measured before UVB exposure. We found that treatment with OMC reduced the peak stress of SC during drying by 24%, while treatment with DOMBM reduced the same by 28% (Fig. 2a). This decrease in peak stress caused by these formulations is likely a result of the same effect of the GTE carrier on lipid interactions.

When specimens treated with GTE are exposed to 265 J cm^{-2} UVB radiation, peak stress levels increase by 10% close to those of untreated SC exposed to UVB radiation, demonstrating an increase in water loss during drying (Fig. 2a). This result shows that any improved lipid compactness or cohesion from the GTE treatment is lost after UVB exposure. This is expected given the importance of ordered lipid lamellae in lipid packing and the lack of any sunscreen molecule in the GTE carrier to prevent the disordering effects of UVB radiation on lipids [14,39].

3.2. Drying stress profiles after sunscreen treatments and UVB exposures

Drying stress profiles for SC treated with OMC and DOMBM sunscreen formulations and exposed to various UVB dosages are shown in Fig. 2 (Fig. 2b and c). In order to better understand the dose effects of UVB radiation on the efficacy of both sunscreens in preventing UVB damage to SC lipids, four UVB dosages were tested between 0 and 265 J cm^{-2}. The observed stress profiles in OMC treated SC increased dramatically to the point of delamination at the 265 J cm^{-2} condition, which is the endpoint of our accelerated damage test (Fig. 2b). In the case of DOMBM treated SC, the stress profiles also increased with increasing UVB exposure, though to a significantly lesser extent than in OMC treated tissue (Fig. 2c). On closer inspection of the peak stresses measured at lower, more physiologically relevant UVB doses, a clear trend is observed in which UVB damage increases rapidly with increasing UVB exposure until some seeming level of saturation is reached at large dosages (Fig. 2a). This result from an accelerated UV degradation experiment indicates that a large part of the lipid damage caused by UVB radiation occurs at physiological dosages, and any further UVB radiation has a smaller effect on lipids in the SC.

In the case of DOMBM treated SC, the observed damage threshold remains constant all the way to the highest used UVB dose of 265 J cm^{-2}, where the measured peak stress is still 10% less than control and 30% less than untreated skin exposed to that level of UVB radiation. OMC treated tissue however, exhibits a sharp deviation from this trend when exposed to 265 J cm^{-2}, showing an increase in peak stress of 19% compared to control. This is a similar level of damage seen in untreated skin exposed to 265 J cm^{-2} of radiation (Fig. 2a). The reduced peak stresses measured in SC treated with OMC and DOMBM formulations and exposed to 5, 30, and 125 J cm^{-2} of UVB light demonstrate that both sunscreen molecules prevent some of the lipid damage caused by UVB radiation. The reduced peak stresses likely indicate that there are still some increased interactions among intercellular lipids due to the presence of GTE. However, the sudden increase of peak stress at high UVB dosage in only the OMC treated SC reveals that the photostability of OMC is inferior to that of DOMBM. Additionally, peak stresses observed in DOMBM treated SC are less than those seen in OMC treated skin at all UVB exposure dosages, illustrating the greater degree of UVB protection afforded by DOMBM [12]. These accelerated damage drying stress measurements indicate that DOMBM is likely a more robust sunscreen molecule at all UVB dosages, even those lower than what was measured here.

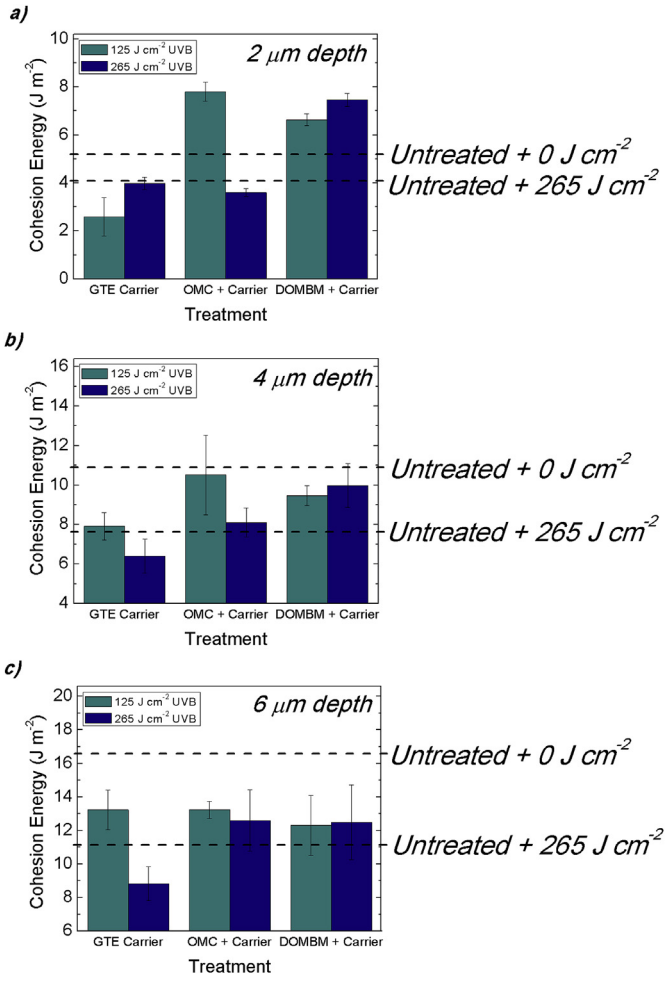

Fig. 3. Comparison of corneocyte cohesion energies of SC specimens treated with the GTE carrier and OMC or DOMBM sunscreen formulations at 125 J cm-2 and 265 J cm-2 UVB exposure conditions. Using the graded delamination technique, measurements were found at depths of **(a)** 2 μm, **(b)** 4 μm, and **(c)** 6 μm beneath the surface of the SC. Dotted lines indicate the G_C values at each depth of SC exposed to 0 and 265 J cm-2 of UVB radiation without any sunscreen treatment.

3.3. Effects of UVB radiation on corneocyte cohesion

Results from depth-fitted corneocyte cohesion tests demonstrating the combined effects on cohesion energy of treatment formulations and various UVB exposures throughout the depth of the SC are shown in Fig. 3 (Fig. 3a, b, c). The raw data of these DCB experiments taken before depth-fitting is shown in Fig. 4, along with the performed linear fit lines (Fig. 4a, b, c). Scatter plots indicating the effect of the depth-fitting technique on measured cohesion energies are also reported in Fig. 4, adjacent to their corresponding raw data plots (Fig. 4d, e, f). Analyzing corneocyte cohesion after sunscreen treatments and UVB exposure indicate changes in the ability of the SC to resist stress induced damage. Without the solar UV protection afforded by many sunscreens, the cohesion energy of SC is typically reduced by UV radiation, meaning it is less resistant to structural damage such as cracking or chapping [6,12]. We observed an expected reduction in cohesion of 1.1 J m^{-2} (21% of control) at a depth of 2 μm beneath the SC surface after 265 J cm^{-2} of UVB exposure (Fig. 3a). Through mobile lipid extraction and enzymatic corneodesmosome (CD) degradation studies, we have previously identified that the main biological components within

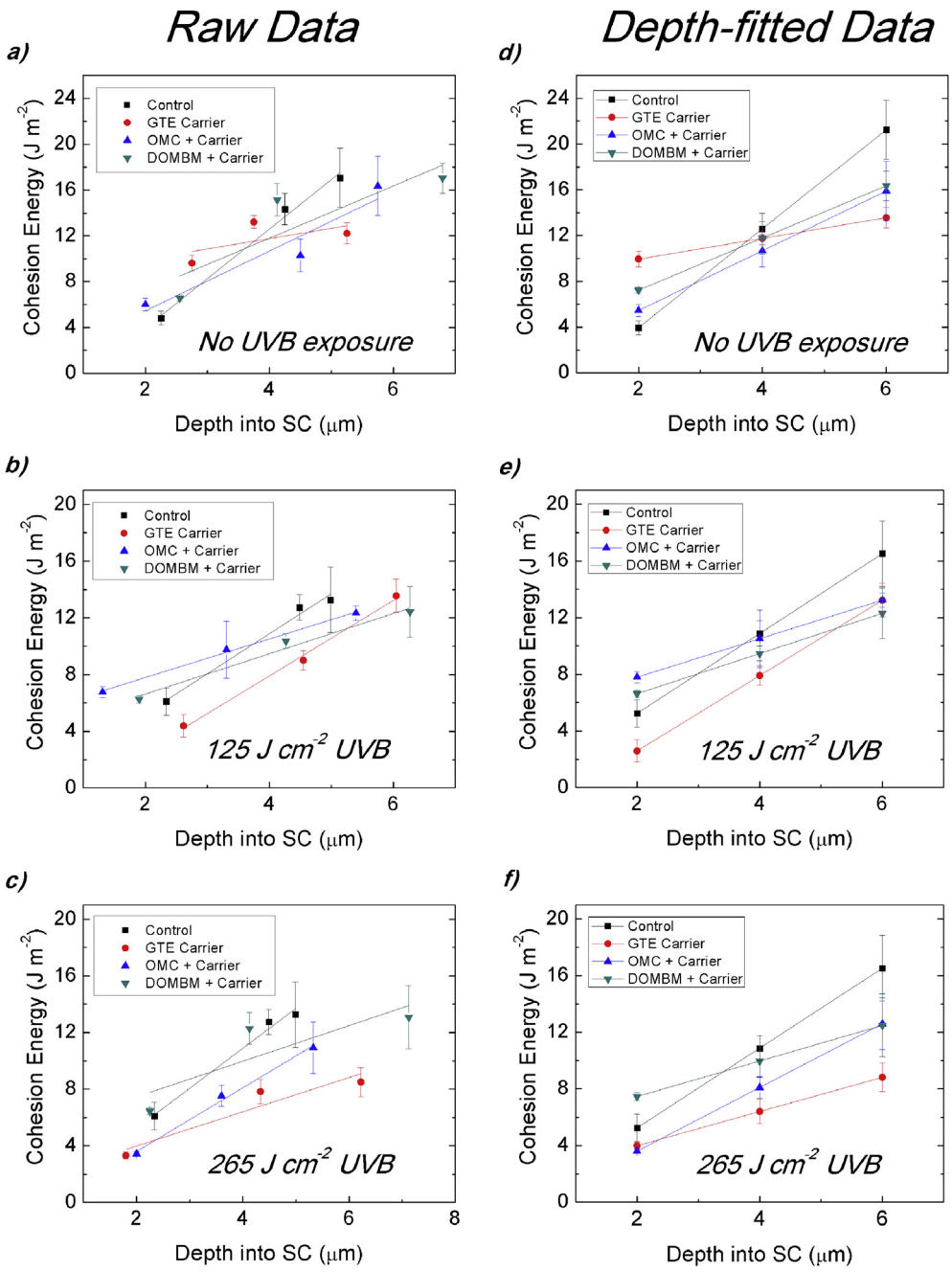

Fig. 4. Raw cohesion energies measured for SC specimens treated with pure GTE carrier, 8wt% OMC in carrier, or 8wt% DOMBM in carrier formulations after UVB exposures of **(a)** 0 J cm^{-2}, **(b)** 125 J cm^{-2}, **(c)** 265 J cm^{-2}. Linear fits of each data set are also shown. Cohesion energies of SC specimens found by interpolating the linear fits of raw data to depths of 2, 4, and 6 μm into the SC surface for **(d)** 0 J cm^{-2}, **(e)** 125 J cm^{-2}, **(f)** 265 J cm^{-2} of UVB exposure.

the SC affecting its cohesion are the CD linkages between corneocytes, with intercellular lipids playing a noticeable role near the SC surface where CD density is lowest [7,42,43]. Thus, the reduced fracture resistance of the SC observed confirms that UVB radiation impairs the mechanical stability of human skin by degrading CD structure, preventing these critical protein junctions from adhering neighboring corneocytes.

Due to the natural process of desquamation, CD density (and consequently SC integrity) increases at deeper layers within the SC [44,45]. Results from our graded delamination technique described above indicate that at 4 μm beneath the SC surface, 265 J cm^{-2} of UVB exposure reduced SC cohesion by 3.2 J m^{-2} (30% of control) (Fig. 3b), and at a depth of 6 μm, cohesion energy dropped by 5.3 J m^{-2} (32% of control) due to the same amount of UVB exposure (Fig. 3c). As observed in previous studies [6,12], the degrading effects of UV radiation on cohesion energy appear to increase deeper into the tissue where CD density is larger, further indicating how UV radiation severely reduces the ability of CDs to provide mechanical integrity to the SC. UV radiation not only affects CDs but can also disrupt the lamellar organization and structure of SC lipids while generating ROS in the skin [39–41]. Lipid damage from UVB radiation may be the cause of the smaller decrease in cohesion of 1.1 J m^{-2} seen 2 μm beneath the SC surface, where the weaker lipid effects on cohesion energy are most noticeable due to low CD density.

3.4. Changes in corneocyte cohesion from sunscreen treatments

The effects of the GTE carrier were measured independently of OMC

or DOMBM sunscreen molecules to ensure any observed changes were not simply due to the presence of an emollient or humectant molecule. We found that treatment with GTE raised the cohesion energy of SC by 6.1 J m^{-2} at a depth of 2 μm into the skin, while deeper measurements at 6 μm into GTE treated tissue revealed a large drop in cohesion of 7.7 J m^{-2} (31% of control) (Fig. 4d). The GTE carrier may be increasing cohesion energy near the top of the SC by improving interactions between lipids covalently bound to corneocyte surfaces. This finding is consistent with observed drying stress results that also demonstrated improved lipid interactions as well as previously published studies showing increases in total cohesion energy due to greater bound lipid cohesion [14,42]. The increased cohesion observed at the surface of SC treated with the GTE carrier also indicates that this molecule is not simply a humectant, as in previous experiments increased hydration levels have always led to decreases in cohesion [7,14]. The reduction in cohesion energy seen deeper into the SC indicates the GTE also contributes to CD degradation, illustrating the large impact this carrier molecule has on multiple SC components.

The 8 wt% OMC and DOMBM in GTE formulations produce effects in the cohesion of SC similar to those of the plain GTE carrier, albeit with reduced impact. DCB measurements at 2 μm beneath the SC surface demonstrate increases in cohesion energy of 1.5 J m^{-2} and 3.3 J m^{-2} in specimens treated with the OMC and DOMBM formulations, respectively. At a depth of 6 μm, the cohesion of SC treated with OMC and DOMBM formulations was reduced by 5.4 J m^{-2} and 4.9 J m^{-2}, respectively (Fig. 4d). These results indicate the sunscreen treatment formulations are also causing an increase in bound lipid interactions while weakening CD linkages between corneocytes. Considering the large effect of the GTE carrier on cohesion, it is likely that the effects of the sunscreen formulations on cellular cohesion were reduced because a lower relative amount of GTE was applied rather than because of any innate action of the sunscreen molecules on CDs or lipids.

3.5. Corneocyte cohesion after combined sunscreen treatments and UVB exposures

The cohesion energies of SC specimens treated with plain GTE and subjected to UVB exposure were then measured to determine any interactions the carrier might have with UVB radiation. When subjected to 265 J cm^{-2} of UVB exposure, the cohesion energy of the SC treated with the GTE carrier dropped by 1.3 J cm^{-2} (24% of control) at a depth of 2 μm (Fig. 3a). Thus, after exposure to UVB radiation, the increase in cohesion seen near the surface of GTE treated tissue has disappeared and been replaced by the expected decrease in surface cohesion due to UVB effects. As seen in drying stress studies, large UVB radiation dosages completely remove any noticeable impact of the GTE carrier. This further indicates that any favorable interactions between bound intercellular lipids mediated by GTE require a distinct lamellar lipid organization. Consequently, when lipid structure and organization are damaged by UVB radiation as discussed previously [39–41], any corresponding increase in G_c is lost and only the typical signs of lipid and CD damage due to UVB exposure are discernible. Measurements taken at 4 μm and 6 μm into the GTE treated tissue exposed to 265 J cm^{-2} of UVB reveal decreases in cohesion energy of 4.5 J cm^{-2} (41% of control) and 7.7 J cm^{-2} (47% of control), respectively (Fig. 3b and c). This decrease in cohesion at greater SC depths is larger than that observed after either UVB exposure or GTE treatments, indicating greater damage to the CD linkages. This suggests that the damaging effects of high UVB exposure and GTE on SC cohesion are cumulative, though whether they are independent effects remains unclear.

Specimens treated with GTE were also subjected to a smaller UVB exposure of 125 J cm^{-2} to determine how the large damage effects seen at the 265 J cm^{-2} dosage scale with the accelerated testing conditions. We found that cohesion energy at 2 μm beneath the surface of GTE treated SC exposed to 125 J cm^{-2} of UVB radiation dropped by 2.7 J m^{-2}, or 51% of control (Fig. 3a). At 4 μm this decrease was 3.0 J m^{-2} or 28% of control (Fig. 3b), and at 6 μm within the SC this decrease was 3.3 J m^{-2} or 20% of control (Fig. 3c). The same reduced cohesion at 2 μm is observed here as in the case of the 265 J cm^{-2} exposure, again indicating a loss of some increased lipid interactions as well as lipid and CD damage. At greater depths into the SC, the reduction in cohesion energy due to combined GTE and UVB exposure actually decreases, which is opposite the trend observed in the case of GTE treated SC exposed to the larger UVB amount of 265 J cm^{-2}. While alone these factors weaken SC integrity through CD degradation, together with a moderate amount of UVB radiation they have a compound effect that leads to a mild reduction in damage. We suggest this may indicate that a small amount of UVB induced crosslinking of GTE and intercellular lipids is occurring to replace partially degraded CDs, though further studies are required to clarify this effect.

Measurements of the cohesion of SC exposed to UVB radiation after treatment with the OMC and DOMBM formulations demonstrate the relative efficacies and photostabilities of these two sunscreen molecules. DCB analysis revealed that at 2 μm beneath the surface, the cohesion energy of OMC treated tissue increased by 49% of control after 125 J cm^{-2} of UVB, while cohesion energy decreased by 31% of control after 265 J cm^{-2} of UVB. At the same tissue depth, the cohesion energy of DOMBM treated tissue increased by 26% of control after 125 J cm^{-2} of UVB, and cohesion energy also increased by 42% of control after 265 J cm^{-2} of UVB (Fig. 3a). At the lower UVB exposure condition, increased cohesion consistent with the effects of the GTE carrier on intercellular lipids can be observed for both sunscreen formulations, indicating the OMC and DOMBM are equally capable of preventing some UVB damage. However, at the higher UVB dosage the GTE effect of increased cohesion is absent in only OMC treated tissue, which instead displays an expected decrease in cohesion due to UVB radiation damage (Fig. 3a). These results from our accelerated damage experiments indicate that there is a significant decline in the effectiveness of OMC while exposed to UVB radiation. This decline in protection is not observed in DOMBM, illustrating the superior photostability of DOMBM to that of OMC.

At a depth of 6 μm into the SC, corneocyte cohesion measurements on OMC treated tissue showed a decrease in cohesion energy of 20% from control when exposed to 125 J cm^{-2} UVB, and a drop of 24% from control when exposed to 265 J cm^{-2}. Similarly, measurements made on DOMBM treated tissue at a depth of 6 μm indicated a reduction in cohesion energy of 25% from control when exposed to 125 J cm^{-2} UVB and a decrease of 24% from control when exposed to 265 J cm^{-2} UVB (Fig. 3c). These reductions in cohesion deeper into the SC are not significantly changed by the amount of UVB exposure whether the applied treatment is OMC or DOMBM. This again demonstrates the complex compound nature of the GTE carrier and UVB interactions described above. While these interactions bear further investigation, both the presence of the GTE carrier along with UVB radiation are weakening the CD linkages throughout the SC, leading to reduced mechanical integrity of the skin.

4. Conclusion

Data obtained through measurements of the SC's inherent mechanical stress and its cohesion energy showed that the biomechanical properties of the SC, which are critical for a robust barrier function of the skin, are strongly affected by not only choice of sunscreen molecules and UVB radiation but also carrier choice. Treatment with the GTE carrier alone caused a reduction in SC stress as well as profound changes in corneocyte cohesion throughout the SC, indicating strong interactions with skin lipids as well as CDs. By studying SC treated with the OMC and DOMBM sunscreen formulations and exposed to various accelerated UVB conditions from the more physiologically relevant to the very large, results from our thin-film techniques illustrated the high photostability of the DOMBM sunscreen and its efficacy at preventing

UVB damage to SC lipids and CDs compared to the OMC sunscreen. This work highlights the need to consider more factors than just the ability of a molecule to block UV radiation when developing commercial sunscreens. The effects of all formulation components on skin biomechanics and stability characteristics of sunscreens are critical in protecting the barrier function of human skin.

Acknowledgements

The authors report no particular acknowledgements. This research did not receive any specific grant from funding agencies in the public, commercial, or not-for-profit sectors.

Transparency document

Transparency document related to this article can be found online at https://doi.org/10.1016/j.bbrep.2019.100657.

References

[1] M. El-Domyati, S. Attia, F. Saleh, D. Brown, D.E. Birk, F. Gasparro, et al., Intrinsic aging vs. photoaging: a comparative histopathological, immunohistochemical, and ultrastructural study of skin, Exp. Dermatol. 11 (2002) 398–405.
[2] A. Kammeyer, R.M. Luiten, Oxidation events and skin aging, Ageing Res. Rev. 21 (2015) 16–29.
[3] S. Seité, C. Medaisko, F. Christiaens, C. Bredoux, D. Compan, H. Zucchi, et al., Biological effects of simulated ultraviolet daylight: a new approach to investigate daily photoprotection, Photodermatol. Photoimmunol. Photomed. 22 (2006) 67–77.
[4] Y. Matsumura, H.N. Ananthaswamy, Toxic effects of ultraviolet radiation on the skin, Toxicol. Appl. Pharmacol. 195 (2004) 298–308.
[5] C. Marionnet, C. Tricaud, F. Bernerd, Exposure to non-extreme solar UV daylight: spectral characterization, effects on skin and photoprotection, Int. J. Mol. Sci. 16 (2015) 68–90.
[6] K. Biniek, K. Levi, R.H. Dauskardt, Solar UV radiation reduces the barrier function of human skin, Proc. Natl. Acad. Sci. 109 (2012) 17111–17116.
[7] K.S. Wu, W.W. Van Osdol, R.H. Dauskardt, Mechanical properties of human stratum corneum: effects of temperature, hydration, and chemical treatment, Biomaterials 27 (2006) 785–795.
[8] K. Levi, R.J. Weber, J.Q. Do, R.H. Dauskardt, Drying stress and damage processes in human stratum corneum, Int. J. Cosmet. Sci. 32 (2010) 276–293.
[9] M.F. Leyva-Mendivil, A. Page, N.W. Bressloff, G. Limbert, A mechanistic insight into the mechanical role of the stratum corneum during stretching and compression of the skin, J. Mech. Behav. Biomed. Mater. 49 (2015) 197–219.
[10] R.M. Lucas, A.J. Mcmichael, B.K. Armstrong, W.T. Smith, Estimating the global disease burden due to ultraviolet radiation exposure, Int. J. Epidemiol. 37 (2008) 654–667.
[11] J. D'Orazio, S. Jarrett, A. Amaro-Ortiz, T. Scott, UV radiation and the skin, Int. J. Mol. Sci. 14 (2013) 12222–12248.
[12] C. Berkey, K. Biniek, R.H. Dauskardt, Screening sunscreens: protecting the biomechanical barrier function of skin from solar ultraviolet radiation damage, Int. J. Cosmet. Sci. 39 (2017) 269–274.
[13] S. Seité, A. Fourtanier, D. Moyal, A.R. Young, Photodamage to human skin by suberythemal exposure to solar ultraviolet radiation can be attenuated by sunscreens: a review, Br. J. Dermatol. 163 (2010) 903–914.
[14] K.S. Wu, M.M. Stefik, K.P. Ananthapadmanabhan, R.H. Dauskardt, Graded delamination behavior of human stratum corneum, Biomaterials 27 (2006) 5861–5870.
[15] K. Levi, R.H. Dauskardt, Application of substrate curvature method to differentiate drying stresses in topical coatings and human stratum corneum, Int. J. Cosmet. Sci. 32 (2010) 294–298.
[16] K. Levi, a. Kwan, a. S. Rhines, M. Gorcea, D.J. Moore, R.H. Dauskardt, Emollient molecule effects on the drying stresses in human stratum corneum, Br. J. Dermatol. 163 (2010) 695–703.
[17] J. Kockler, M. Oelgemöller, S. Robertson, B.D. Glass, Photostability of sunscreens, J. Photochem. Photobiol. C Photochem. Rev. 13 (2012) 91–110.
[18] R.C. Romanhole, J.A. Ataide, L.C. Cefali, P. Moriel, P.G. Mazzola, Photostability study of commercial sunscreens submitted to artificial UV irradiation and/or fluorescent radiation, J. Photochem. Photobiol. B Biol. 162 (2016) 45–49.
[19] J.M. Allen, C.J. Gossett, Photochemical formation of singlet molecular oxygen in illuminated aqueous solutions of several commercially available sunscreen active ingredients, Chem. Res. Toxicol. 9 (1996) 605–609.
[20] L.R. Gaspar, P.M.B.G. Maia Campos, Evaluation of the photostability of different UV filter combinations in a sunscreen, Int. J. Pharm. 307 (2006) 123–128.
[21] I. Karlsson, L. Hillerström, A.L. Stenfeldt, J. Mårtensson, A. Börje, Photodegradation of dibenzoylmethanes: potential cause of photocontact allergy to sunscreens, Chem. Res. Toxicol. 22 (2009) 1881–1892.
[22] H. Gonzalez, N. Tarras-Wahlberg, B. Strömdahl, A. Juzeniene, J. Moan, O. Larkö, et al., Photostability of commercial sunscreens upon sun exposure and irradiation by ultraviolet lamps, BMC Dermatol. 7 (2007) 1.
[23] R. Jiang, M.S. Roberts, D.M. Collins, H.A.E. Benson, Absorption of sunscreens across human skin: an evaluation of commercial products for children and adults, Br. J. Clin. Pharmacol. 48 (1999) 635–637.
[24] J. Schulz, H. Hohenberg, F. Pflücker, E. Gärtner, T. Will, S. Pfeiffer, et al., Distribution of sunscreens on skin, Adv. Drug Deliv. Rev. 54 (2002) 157–163.
[25] T. Haque, J.M. Crowther, M.E. Lane, D.J. Moore, Chemical ultraviolet absorbers topically applied in a skin barrier mimetic formulation remain in the outer stratum corneum of porcine skin, Int. J. Pharm. 510 (2016) 250–254.
[26] N.R. Janjua, Ã.B. Mogensen, Ã.A. Andersson, H. Petersen, Ã.N.E. Skakkebæk, H.C.W. Ã, Systemic absorption of the sunscreens benzophenone-3, octyl-methoxycinnamate, and 3-(4-methyl-benzylidene)camphor after whole-body topical application and reproductive hormone levels in humans, J. Investig. Dermatol. 123 (2004) 57–61.
[27] M.M. Jiménez, J. Pelletier, M.F. Bobin, M.C. Martini, Influence of encapsulation on the in vitro percutaneous absorption of octyl methoxycinnamate, Int. J. Pharm. 272 (2004) 45–55.
[28] S.T. Butt, T. Christensen, Toxicity and phototoxicity of chemical sun filters, Radiat. Protect. Dosim. 91 (2000) 283–286.
[29] S. Pattanaargson, T. Munhapol, P. Hirunsupachot, P. Luangthongaram, Photoisomerization of octyl methoxycinnamate, J. Photochem. Photobiol. A Chem. 161 (2004) 269–274.
[30] F.P. Gasparro, M. Mitchnick, J.F. Nash, A review of sunscreen safety and efficacy, Photochem. Photobiol. 68 (1998) 243–256.
[31] A. Kikuchi, S. Yukimaru, N. Oguchi, K. Miyazawa, M. Yagi, Excited triplet state of a UV-B absorber, Octyl Methoxycinnamate, Chem. Lett. 39 (2010) 633–635.
[32] N. Oguchi-Fujiyama, K. Miyazawa, A. Kikuchi, M. Yagi, Photophysical properties of dioctyl 4-methoxybenzylidenemalonate: UV-B absorber, Photochem. Photobiol. Sci. 11 (2012) 1528.
[33] K. Biniek, A. Tfayli, R. Vyumvuhore, A. Quatela, M.F. Galliano, A. Delalleau, et al., Measurement of the biomechanical function and structure of ex vivo drying skin using Raman spectral analysis and its modulation with emollient mixtures, Exp. Dermatol. 27 (2018) 901–908.
[34] C.H. Lee, S.B. Wu, C.H. Hong, H.S. Yu, Y.H. Wei, Molecular mechanisms of UV-induced apoptosis and its effects on skin residential cells: the implication in UV-based phototherapy, Int. J. Mol. Sci. 14 (2013) 6414–6435.
[35] ASTM, Standard Tables for Reference Solar Spectral Irradiances: Direct Normal and Hemispherical on 37° Tilted Surface vol 03, ASTM, 2013, pp. 1–21.
[36] M.F. Kanninen, An augmented double cantilever beam model for stud propagation and arrest, Int. J. Fract. 9 (1973) 83–92.
[37] R. Vyumvuhore, A. Tfayli, K. Biniek, H. Duplan, A. Delalleau, M. Manfait, et al., The relationship between water loss, mechanical stress, and molecular structure of human stratum corneum ex vivo, J. Biophot. 9 (2014) 1–9.
[38] R.O. Potts, M.L. Francoeur, The influence of stratum corneum morphology on water permeability, J. Investig. Dermatol. 96 (1991) 495–499.
[39] S. Meguro, Y. Arai, K. Masukawa, K. Uie, I. Tokimitsu, Stratum corneum lipid abnormalities in UVB-irradiated skin, Photochem. Photobiol. 69 (1999) 317–321.
[40] Y. Shindo, E. Witt, D. Han, L. Packer, Dose-response effects of acute ultraviolet irradiation on antioxidants and molecular markers of oxidation in murine epidermis and dermis, J. Investig. Dermatol. 102 (1994) 470–475.
[41] A. Svobodova, D. Walterova, J. Vostalova, Ultraviolet light induced alteration to the skin, Biomed. Pap. Med. Fac. Univ. Palacky Olomouc Czech Repub. 150 (2006) 25–38.
[42] K.S. Wu, J. Li, K.P. Ananthapadmanabhan, R.H. Dauskardt, Time-dependant intercellular delamination of human stratum corneum, J. Mater. Sci. 42 (2007) 8986–8994.
[43] K. Levi, J. Baxter, H. Meldrum, M. Misra, E. Pashkovski, R.H. Dauskardt, Effect of corneodesmosome degradation on the intercellular delamination of human stratum corneum, J. Investig. Dermatol. 128 (2008) 2345–2347.
[44] J.W. Fluhr, J. Kao, M. Jain, S.K. Ahn, K.R. Feingold, P.M. Elias, Generation of free fatty acids from phospholipids regulates stratum corneum acidification and integrity, J. Investig. Dermatol. 117 (2001) 44–51.
[45] M. Simon, D. Bernard, A.M. Minondo, C. Camus, F. Fiat, P. Corcuff, et al., Persistence of both peripheral and non-peripheral corneodesmosomes in the upper stratum corneun of winter xerosis skin versus only peripheral in normal skin, J. Investig. Dermatol. 116 (2001) 23–30.